Citation: **Hirt C,** Featherstone WE (2012) A 1.5 km-resolution gravity field model of the Moon. *Earth Planet Science Letters (EPSL),* 329-330, 22-30, DOI: 10.1016/j.epsl.2012.02.012.

A 1.5km-resolution gravity field model of the Moon

C. Hirt*

Western Australian Centre for Geodesy & The Institute for Geoscience Research,

Curtin University of Technology, GPO Box U1987, Perth, WA 6845, Australia

Email: c.hirt@curtin.edu.au

Fax: +61 8 9266 2703

Tel:+61 8 9266 7559

W.E. Featherstone

Western Australian Centre for Geodesy & The Institute for Geoscience Research,

Curtin University of Technology, GPO Box U1987, Perth, WA 6845, Australia

Email: w.featherstone@curtin.edu.au

Fax: +61 8 9266 2703

Tel:+61 8 9266 2734

* corresponding author

Abstract

We present a high-resolution lunar gravity field model (LGM2011) that provides gravity accelerations, free-air gravity anomalies, selenoid undulations and vertical deflections over the entire Moon's surface. LGM2011 is based on the Japanese SELENE mission that provides the low- and medium-frequency constituents of the gravity field, down to spatial scales of ~78 km. At spatial scales between ~78 km and ~1.5 km, LGM2011 uses high-frequency topographic information derived from LOLA laser altimetry to approximate the gravity field signatures of many medium- and small-size impact craters for the first time. For the topography-based gravity approximation, we use Newtonian forward-modelling under the key assumptions that the SELENE and LOLA data are consistent, the high-frequency lunar topography is uncompensated and the topographic mass density is constant. The short-scale component of LGM2011 should not be relied upon in geophysical interpretations. LGM2011 can be used as an a priori model for lunar gravity field simulation and inversion studies, evaluation of past and future lunar gravity field missions, improved topographic mapping,

lunar inertial navigation, and the prediction of lunar gravity acceleration and vertical deflections at any future landing sites.

Key words

Moon, gravity, topography, forward-modelling, selenoid

1 Introduction

Precise knowledge of the lunar gravity field contributes to understanding the evolution and structure of the Moon (e.g., Konopliv et al., 1998; Matsumoto et al., 2010), navigation of space vehicles (e.g., Sinha et al., 2010), topographic mapping (e.g., Wieczorek, 2007), and modelling of orbit perturbations in lunar laser altimetry (e.g., Rowlands et al., 2009; Mazarico et al., 2010). A number of medium-resolution lunar gravity field models have been developed based on two-way tracking data to artificial lunar satellites. One shortcoming of such lunar gravity field models (Konopliv et al., 2001; Mazarico et al., 2010; Sinha et al., 2010) based on orbit analysis of NASA's Lunar Prospector (LP) and other spacecrafts is the lack of far-side observations. This is because the synchronised rotation and revolution of the Moon prevents two-way tracking of lunar satellites over the far-side (Konopliv et al., 2001).

Recently, however, knowledge of the far-side gravity field has been improved through four-way tracking data from the Japanese SELENE (Selenological and Engineering Explorer, or Kaguya) mission using relay satellites (Namaki et al., 2009; Goossens et al, 2011). The most recent SELENE gravity field models, SGM100i (Goossens et al., 2011) and SGM100h (Matsumoto et al., 2010), reliably resolve the lunar gravity field to spherical harmonic degree and order ~70 (equivalent to spatial scales of ~78 km) with a formal model resolution to degree and order 100 (spatial scales of ~55 km), cf. Matsumoto et al. (2010). More recently, LP radio tracking data was re-analysed to resolve near-side gravity anomalies down to scales of 30 km (Han et al., 2011).

Common to any space-collected lunar gravity field model is that gravity attenuation at satellite altitude limits the model resolution (e.g., Kaula, 1966). In the case of SELENE models, structures at scales less than ~78 km are only partially captured, whilst scales less than ~55 km are omitted (Matsumoto et al., 2010). Hence, the gravitational signatures of small-scale impact craters remain partially or completely unresolved. Some LP-based gravity field models reach resolutions beyond degree 100 over the near-side (Konopliv et al., 2001; Mazarico et al., 2010; Han et al., 2011), but not over the entire far-side. Regional refinements from line-of-sight acceleration data (Sugano and Heki, 2004a) and orbit residuals (Goossens

et al., 2005) have been reported. However, none is capable of resolving the high-frequency gravity field at scales of few km to tens of km over the entire lunar surface. As will be shown here, the short-scale lunar gravity field reaches amplitudes that are significant for a range of gravity field applications.

On Earth, high-frequency gravity signals are modelled based on surface gravity observations and digital elevation models (DEMs). While the few lunar surface gravity measurements (Nance, 1969; Talwani, 2003) are far too scarce for detailed gravity field modelling, high-resolution lunar DEMs are now available based on laser altimetry (Araki et al., 2009; Smith et al., 2010). DEMs are a convenient data source for improving the spatial resolution of gravity field models in the absence of surface gravity observations (Hirt et al., 2010a). This is because topographic masses generate a major part of the high-frequency gravity signal on Earth (Forsberg and Tscherning, 1981), the Moon and terrestrial planets (Wieczorek, 2007), so are a valuable source for Newtonian forward-modelling (Forsberg, 1984; Pavlis et al., 2007; Hirt, 2010) to construct high-resolution gravity models.

2. Data and methods

LGM2011 (Lunar Gravity Model 2011) is a composite of three different input data sets that take into account or depend upon the lunar topography (Section 2.1). First, SELENE delivers the low- and medium-frequency constituents of the gravity field, reliably to spatial scales of ~78 km (Section 2.2). Second, Newtonian forward-modelling is used to create a high-frequency topography-implied gravity field that resolves spatial scales to ~1.5 km (Section 2.3), whereby high-resolution elevation data from the Lunar Orbiter Laser Altimeter (LOLA, cf. Smith et al., 2010), operated on the operated on the Lunar Reconnaissance Orbiter (LRO, cf. Vondrak et al., 2010), is used. Finally, normal gravity is modelled to take into account the gravitational attraction of the Moon's total mass and the decay of gravity with height (Section 2.4).

Our forward gravity modelling is based on the key assumptions of (1) coherence of SELENE and LOLA, (2) uncompensated high-frequency topography and (3) a constant mass-density. All constituents are computed on 1/20° grids (25.92 million points), equivalent to a ~1.5 km spatial resolution at the lunar equator. LGM2011 is based on tested strategies used to refine Earth gravity field models at short spatial scales (Forsberg, 1984; Forsberg and Tscherning, 1981; Pavlis et al., 2007; Hirt, 2010; Hirt et al., 2010a, 2010b, 2011).

LGM2011 combines data from two different missions. It implicitly assumes the SELENE and LRO mission results to be consistent, in terms of the selenocentric coordinates

used to represent the SELENE gravity field and LOLA elevations, and orbits involved in deriving the two data sets. The high-degree component and its continuation down to scales of ~1.5 km is thus assumed to be relatively immune from biases and errors generated by the use of laser altimetry data not necessarily matching the gravity (and therefore orbit) data. In such a combination, the assumption that these data are coherent has to be made.

2.1 Lunar topography

As a high-resolution DEM of the lunar topography, we use the LOLA-3 release from the LOLA altimeter (Smith et al., 2010). Given LOLA's ~18 m along-track and current ~1.8 km across-track spacing at the lunar equator (Smith et al., 2010), 1/20° (~1.5 km) resolution is suitable. The 1/64° resolution LOLA-3 elevation product (LRO-L-LOLA-3-GDR-V1.0), available via http://pds-geosciences.wustl.edu/missions/lro/lola.htm, was used to derive the 1/20° resolution through bicubic interpolation. This 1/20° LOLA elevation grid is utilised consistently in the computation of all three LGM2011 constituents (Sections 2.2 – 2.4).

2.2 SELENE evaluation

SGM100i (Goossens et al. 2011; http://www.soac.selene.isas.jaxa.jp/archive/) was selected as the source for the low- and medium-frequency signals for LGM2011 to spherical harmonic degree and order 70. Though resolving the lunar gravity field beyond degree 100 over the near-side, we did not use LP-based models in the construction of LGM2011 because of the known deficiencies over the lunar far-side (Konopliv et al., 2001; Mazarico et al., 2010; also see the Introduction).

Goossens et al. (2011, Fig.13) show that the correlation between lunar topography and SGM100i-implied gravity deteriorates rapidly beyond degree 70, demonstrating that the current SELENE-based models are underpowered at short scales. That is, they do not fully resolve the topography-induced gravity field signal at scales less than ~78 km. Our truncation of SGM100i to degree-70 may give rise to Gibbs effects and other artefacts because of the correlations between the harmonic coefficients.

We used SGM100i to degree 70 for synthesis of SGM100i gravity accelerations, computed as radial derivatives of the gravitational potential ($\partial V/\partial R$) with software based on the harmonic_synth program (Holmes and Pavlis, 2008). The $\partial V/\partial R$ are also known as gravity disturbances (e.g., Torge, 2001). Based on our experiences in Earth-based gravity field modelling (Hirt et al. 2010a), we evaluated SGM100i at the topographic surface, as represented by the LOLA DEM, and not at the surface of some mean-Moon sphere with

constant radius. Such synthesis at the topography takes into account the effect of gravitational field-strength decay with height, as corroborated with ground-truth comparisons on Earth (Hirt et al. 2010a).

2.3 Newtonian forward-modelling

A forward-modelling procedure based on Newton's law of gravitation was used to estimate the high-frequency lunar gravity field not represented by SGM100i. DEMs such as LOLA-3 provide a source of long- to short-wavelength gravity field signals (cf. Wieczorek, 2007). To avoid double modelling, we subtracted a smooth reference surface from the LOLA topography. As a commensurate reference, we use the degree-70 spherical harmonic expansion of the LOLA topography (Smith et al., 2010). This harmonic filtering procedure (Hirt 2010) removes most parts (above 90%) of the SGM100i-sensed topographic signals from LOLA (cf. Hirt et al. 2010a).

This high-pass filtered LOLA DEM can be considered and treated as a residual topography model (RTM; Forsberg, 1984) for high-frequency Newtonian forward-modelling to augment SGM100i. The LOLA RTM elevations represent elementary mass-prisms of constant mass-density that are converted to gravity accelerations by closed-form expressions for Newtonian forward-modelling. The equations are found in, e.g., Forsberg and Tscherning (1981), Forsberg (1984), Nagy et al. (2000), so are not duplicated here. Empirical results by Hirt (2010); Hirt et al. (2010a, 2011) demonstrate that Newtonian forward-modelling based on RTM data, as obtained from harmonically filtered elevations, is most suitable to augment spherical harmonic gravity models beyond their resolution in the cases of no surface gravity data.

Our forward-modelling relies on the key assumptions of isostatically uncompensated topography and a constant mass-density. The uncompensated topographic masses can be thought to increasingly dominate the lunar gravity field at finer spatial scales, as we infer from Mazarico et al., (2010, Fig. 8 ibid), and Goossens et al., (2011, Fig. 13 ibid, and section 4.3.2. ibid). Goossens et al. (2011) analysed the correlation between uncompensated topography and SELENE gravity over the far-side and found correlation coefficients ranging between ~+0.90 to ~+0.95 (ibid, Fig. 13) at spatial scales of ~109 to ~78 km, corresponding to harmonic degrees 50 to 70. Mazarico et al. (2010, section 3.5.3 ibid) used topography to constrain the least-squares inversion of their gravity field solution [at short wavelengths], whereby the topography was considered uncompensated. Mazarico et al. (2010, Fig. 8 ibid) quantified the correlation between uncompensated topography and LP-derived gravity over

the near-side with about +0.9 for scales of ~100 km down to ~50 km (harmonic degrees ~60 to ~110), and found correlation coefficients in excess of +0.95 for a selected [rugged and cratered] region over the near-side. Our forward-modelling approximates the expected fine-structure of the lunar gravity field, and is not capable of delivering information on anomalous field signatures, as could be caused from isostatic compensation of medium-sized craters, or anomalies where the actual mass-density deviates from the modelled mass-density. Correlation coefficients never quite reaching +1.0 in the above-cited works can be related to isostatic compensation effects. The isostatic state of the Moon is not the main topic of this contribution, for past results see, e.g., Watts (2001), p 384ff.; Reindler and Arkani-Hamad,(2001); Sugano and Heki, (2004b).

It is reasonable to expect that small-scale topographic features, say at few km to ~10 km scales, are widely supported by the lunar crust. This is "*because short-wavelength loads on the elastic lithosphere will not produce significant bending and compensation, the observed gravitational signal will be closely related to the topography, except in zones with local tectonics. Thus, a large correlation coefficient at high degrees is usually interpreted as a sign of quality of the gravity field, accurately reproducing the signal of mostly uncompensated topography*" (Mazarico et al. 2010, Sect 3.4.1 ibid).

We configured a variant of the TC software (Forsberg, 1984) for lunar mass-density modelling by using Moon constants (radius of 1738 km, mean gravity of 1.62 m/s^2) in place of Earth constants. The gravitational functionals of the RTM topography were computed using rectangular mass-prisms (Forsberg and Tscherning, 1981, Nagy et al., 2000) in planar approximation as represented by the LOLA RTM elevations. For each computation point, we numerically integrated the gravitational potential of all mass-prisms within a circular zone of 400 km radius from each computation point. This radius is suitable because the lowest frequencies contained in the LOLA RTM are at scales of ~78 km or greater. Effects of prisms outside this zone can be neglected given the oscillating character of the RTM topography and attenuation of gravitational attraction with increasing distance (Forsberg, 1984; Hirt, 2010; Hirt et al., 2010a).

For the evaluation of mass-prism effects at high selenocentric latitudes (beyond 70° north or south), the LOLA RTM grid was rotated towards the equator. The Newtonian forward-modelling was carried out at 25.92 million (3600 x 7200) grid points, requiring a total computation time of ~12 days on a quad-core PC platform.

The topography-implied gravity field component, which we call LRTM70 (Lunar RTM gravity field with the spectrum to degree 70 removed) and abbreviate to Newtonian

gravity in the sequel, augments SGM100i. We assume a constant value of 2800 kg m^{-3} (Wieczorek, 2007; Matsumoto et al., 2010) for the mass-density of the residual topography. Because of this constant mass-density assumption, our Newtonian gravity only ever approximates the short-scale gravity field signatures. Local mass-density anomalies are not taken into account because sufficiently detailed topographic density maps of the Moon are not available. Given the linear relation between gravity and mass-density (e.g., Nagy et al., 2000), the error of our Newtonian gravity is estimated to be ~10 % in cases of mass-densities for the upper crustal material of mare deposits of ~3100 kg m^{-3} (Wieczorek, 2007). Over areas with ~2900 kg m^{-3} crustal mass-density, our Newtonian gravity would be in ~3 % error.

In Earth gravity field modelling, constant mass-density forward-modelling has been shown to be a very effective method to estimate the short-scale gravity field in rugged terrain (Pavlis et al., 2007; Hirt 2010). Newtonian gravity, modelled at spatial scales between ~10 km and ~100 m, improved the agreement between measured and spherical harmonic gravity by ~89 % over the Swiss Alps (Hirt et al., 2011). It is therefore reasonable to infer that our Newtonian gravity approximates the high-frequency lunar gravity field well.

2.4 Lunar normal gravity

The role of the lunar normal gravity field is to account for those parts that are generated by the Moon's total mass, including their decay with height (i.e., the free-air effect in Earth-based parlance). We have designed the lunar normal gravity field based on current 'best-estimates' for GM (product of the lunar mass and the universal gravitational constant) and the mean radius of the Moon.

We use GM = 4902.80080 x 10^9 m^3s^{-2} from SGM100i (Goossens et al., 2011) and R = 1737153 m from LOLA (Smith et al. 2010), ω = 0.26616995 x 10^{-5} rad s^{-1} for angular velocity of the Moon's rotation (Sagitov et al., 1986). The geometric flattening is assumed to be zero, since the moon is more spherical than elliptical (Seidelmann et al., 2002; JPL, 2005).

From these defining parameters, the lunar normal gravity is $\gamma_0 = GM/R^2$ =1.624681 ms^{-2} (at the surface of radius R = 1737153 m), the first-order free-air gradient $\partial\gamma/\partial R = -2\gamma/R$ = – 1.8705 x 10^{-6} s^{-2} and the second-order free-air gradient $\partial^2\gamma/\partial R^2 = 6\gamma/R^2$ =3.23 x 10^{-12} $m^{-1}s^{-2}$, and the centrifugal acceleration at the equator is $z = \omega^2 R$=1.23 x 10^{-5} ms^{-2}. We thus evaluated the normal gravity at the lunar surface using

$$\gamma \approx \gamma_0 + H\,\partial\gamma/\partial R + H^2/2\,\partial^2\gamma/\partial R^2 - z\cos(\varphi)$$

where H are the LOLA-elevations, relative to R, and φ is selenocentric latitude of the points. The normal gravity field approximates the Moon as homogeneous mass-sphere and not as mass-ellipsoid. The small effect of the lunar geometric flattening (neglected in the normal field) is absorbed by the zonal harmonic coefficients of the SGM100i gravity model. We acknowledge that other estimates of the lunar GM and R have been published (e.g., GM = 4902.8010076 x 10^9 m^3s^{-2} (Konopliv et al., 2001) and R = 1737156.3 m (Araki et al., 2009). However, for the purpose of normal gravity computation, the differences are well below the 10^{-5} ms^{-2} level, and as such negligibly small.

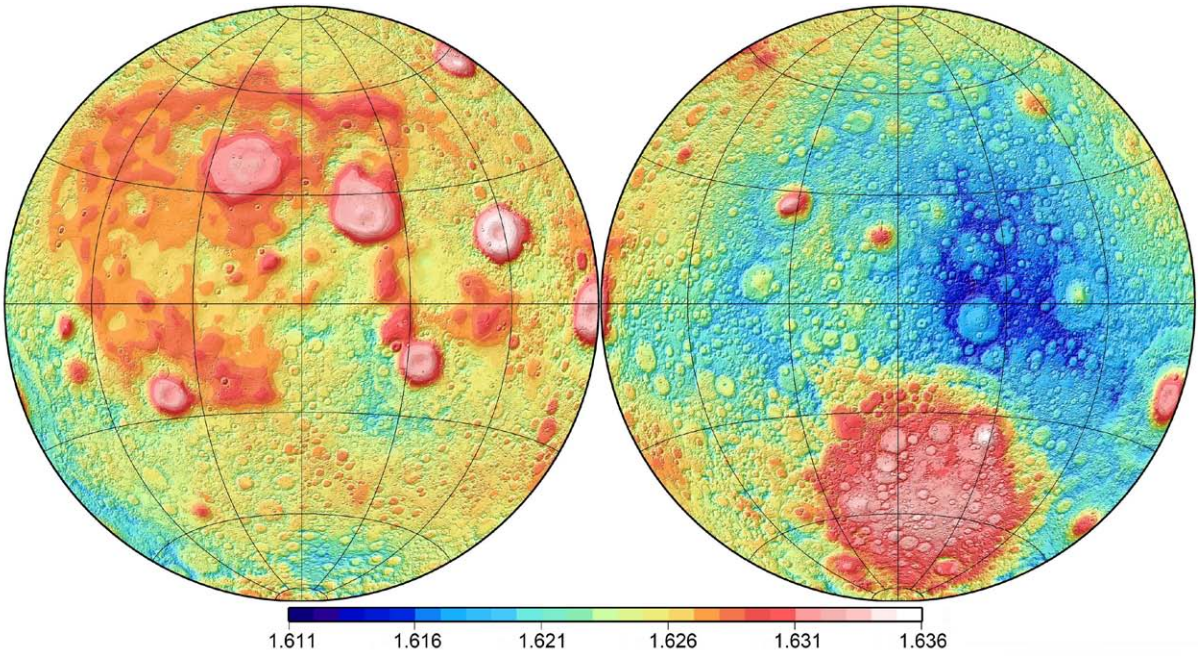

Figure 1. LGM2011 gravity accelerations at the lunar surface (ms^{-2}). The near-side is shown on the left, the far-side on the right. Azimuthal equidistant projection with a central meridian of 0° longitude (left) and 180° (right). Meridians and parallels are 30° apart.

3. LGM2011 gravity

LGM2011 surface gravity accelerations (Fig. 1) are the sum of degree-70 SGM100i gravity (Section 2.2), Newtonian gravity (Section 2.3) and normal gravity (Section 2.4). Over the entire lunar surface, the mean LGM2011 surface gravity acceleration is 1.62486 ms^{-2} and the range is ~0.0253 ms^{-2} (1.6%). The extreme values of lunar surface gravity are located on the far-side: The minimum of 1.61064 ms^{-2} is on the rim of Engelhard (far-side highlands, at 6.1°N, 159.2°W). The maximum of 1.63594 ms^{-2} is at the bottom of a small impact crater (37.5°S, 151.4°W) in Apollo. Gravity highs often occur at the centres of impact craters due to welding and compacting by high-velocity impacts, and because of the free-air effect (Section

2.4). LGM2011 free-air gravity anomalies (Fig. 2) are the sum of Newtonian and SGM100i, which reflect those parts of the lunar mass distribution that depart from a sphere of homogeneous density. The variation range of free-air gravity anomalies is ~0.0156 ms^{-2}, the average signal strength is ~0.0015 ms^{-2} (Table 1).

The three LGM2011 gravity input data sets: Newtonian gravity (LRTM70), SGM100i and normal gravity are shown in Fig. 3. The Newtonian gravity (Fig. 3A) resolves the (expected) signatures of numerous impact craters and other topographic features such as rilles and domes, grabens and wrinkle ridges. The SGM100i spectral band 2 to 70 (Fig. 3B) models many features of the lunar gravity field that are not implied by the topography alone, such as mass concentrations in the lunar mare (cf. Goossens et al., 2011).

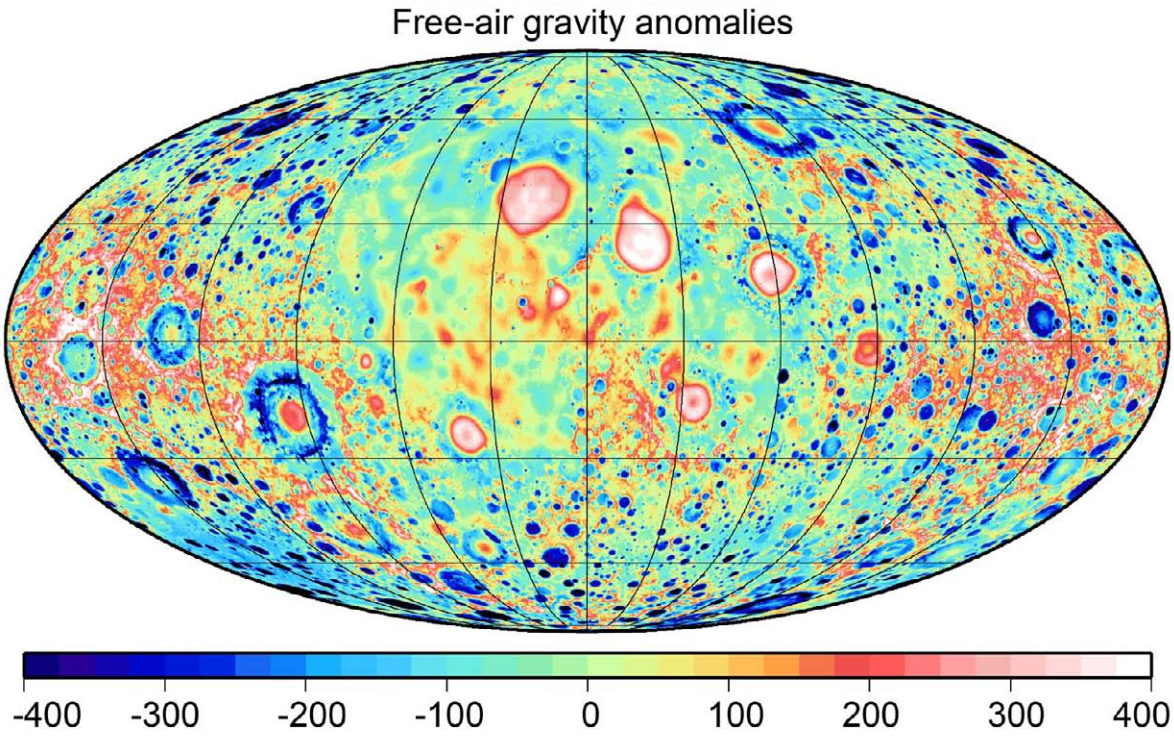

Figure 2. LGM2011 free-air gravity anomalies (10^{-5} ms^{-2}). The near-side is shown in the centre, the far-side on the left and right. Mollweide projection with a central meridian of 0° longitude. Meridians and parallels are 30° apart.

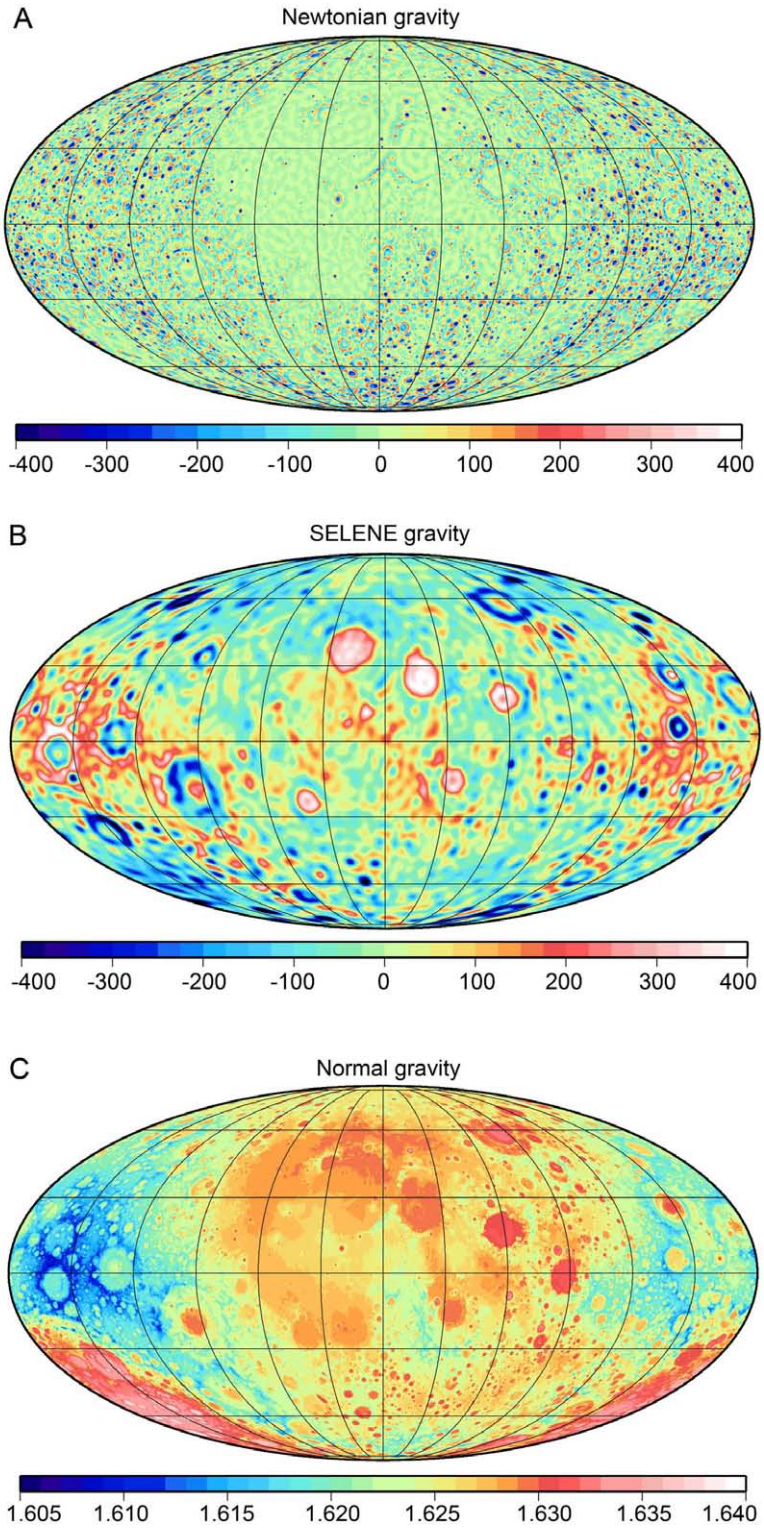

Figure 3. LGM2011 input data. A: Newtonian gravity (LRTM70). B: SELENE free-air gravity anomalies (model SGM100i, evaluated at the LOLA-topography in spectral band 2 to 70). C: Normal gravity (evaluated at the LOLA topography). Units of panels A and B are 10^{-5} ms^{-2}, units of panel C is ms^{-2}. Mollweide projection with a central meridian of 0° longitude. Meridians and parallels are 30° apart.

Table 1. Descriptive statistics of LGM2011 surface gravity and LGM2011 free-air anomalies and of the three input components LRTM70, SGM100i (band 2 to 70) and the normal gravity field. Units in 10^{-5} ms^{-2}. STD = Standard deviation.

Functional	**Min**	**Max**	**Mean**	**STD**
LGM2011 surface gravity acceleration	161064	163594	162486	342
LGM2011 free-air gravity anomalies	-890	671	-33	154
LRTM70 (Newtonian gravity)	-767	603	-10	99
SGM100i (SELENE free-air gravity anomalies in spectral band 2 to 70)	-647	528	-23	117
Normal gravity acceleration	160430	164138	162519	412

From Table 1, the LRTM70 Newtonian gravity signal has a commensurate strength to SGM100i in spectral bands 2 to 70, while the variation range (max minus min) of the Newtonian is larger than SGM100i component. This demonstrates that – without Newtonian augmentation by LRTM70 – a degree-70 tracking-only lunar gravity field (exemplified by SGM100i) omits roughly half of the total lunar gravity field signal. Localised images of LGM2011 gravity constituents (Fig. 4) demonstrate the limited resolution of SGM100i and the gain in spatial resolution obtained through Newtonian forward-modelling. LRTM70 (Fig. 4A), that relies on the assumption of uncompensated and constant mass-density topography, resolves the expected signatures of numerous small-scale impact craters.

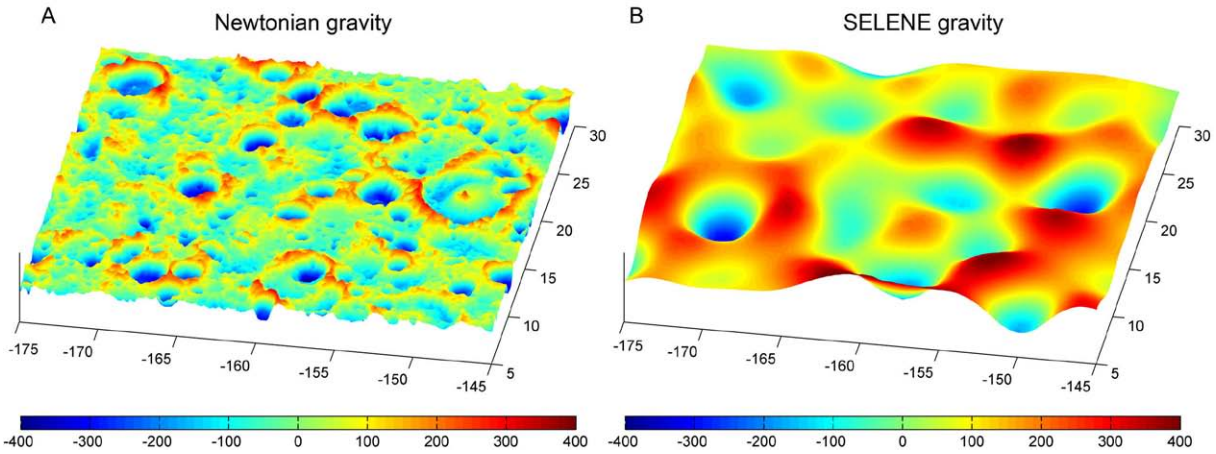

Figure 4. 3D-views of LGM2011 input data (30°x25° area over the lunar far-side). A: Newtonian gravity (LRTM70). B: SELENE gravity (SGM100i evaluated at the LOLA-topography in spectral band 2 to 70). Units in 10^{-5} ms^{-2}.

4. LGM2011 by-products

We have derived – as by-products – LGM2011 and LRTM70 selenoid undulations and vertical deflections. Akin to the geoid on Earth, the selenoid is an equipotential surface of the Moon's gravity field at which – if it were present – water would occupy. The LGM2011 and LRTM70 vertical deflections are the horizontal gradients of the selenoid in north-south and east-west directions.

Following the principles applied in the LGM2011 gravity construction, LGM2011 selenoid undulations are the sum of SGM100i (band 2 to 70) gravitational potential V divided by normal gravity V/γ_0 and LRTM70 selenoid undulations, derived from the RTM potential divided by normal gravity. SGM100i selenoid undulations were evaluated at a constant radius R of 1738000 m. From Table 2, most of the LGM2011 selenoid signal is generated by SGM100i (207 m STD, ~550 m maximum value). Newtonian forward-modelling makes a smaller contribution (9 m STD, ~50 m maximum values). This is as expected, given that the spectral power of the selenoid is concentrated in the long- and medium wavelengths (e.g., Torge, 2001).

Table 2. Descriptive statistics of LGM2011, SGM100i and LRTM70 selenoid undulations. Units in metres.

Functional	**Min**	**Max**	**Mean**	**STD**
LGM2011 selenoid	-539	566	-84	207
SGM100i selenoid (band 2 to 70, evaluated at R=1738km)	-532	579	-83	207
LRTM70 selenoid (Newtonian forward-modelling)	-55	51	0	9

LGM2011 vertical deflections are provided in North-South (NS) and East-West (EW) directions at the lunar surface. Similarly to surface gravity, LGM2011 vertical deflections were constructed as the sum of SGM100i (band 2 to 70, evaluated at the LOLA topography) and LRTM70 vertical deflections. LGM2011 vertical deflections are the horizontal derivatives of the lunar gravitational potential V. The LGM2011 NS vertical deflection is computed as $-\partial V/\partial\varphi/(\gamma_0 R)$ and the EW deflection as $-\partial V/\partial\lambda/(\gamma_0 R\cos\varphi)$, where λ is the selenocentric longitude. To account for the attenuation of gravity with height, SGM100i was evaluated at the surface of the LOLA topography. This procedure parallels successful experiments on Earth: over the European Alps, observed vertical deflections were in close

agreement with vertical deflections from a gravity model (synthesized at the height of the topography) and Newtonian forward-modelling (Hirt et al., 2010b).

Fig. 5 shows the magnitude of LGM2011 vertical deflections over the entire lunar surface. The strength of LGM2011 vertical deflections is ~130 arc seconds with maximum values of ~930 arc seconds (Table 3). The two input components SGM100i (band 2 to 70) and LRTM70 have comparable signal strengths (~90 arc second STD), showing that vertical deflections – as derivatives of the potential – possess similar spectral power at all scales. As was the case for LGM2011 surface gravity, roughly half of the vertical deflection signal would be omitted if Newtonian forward-modelling (LRTM70) were not applied.

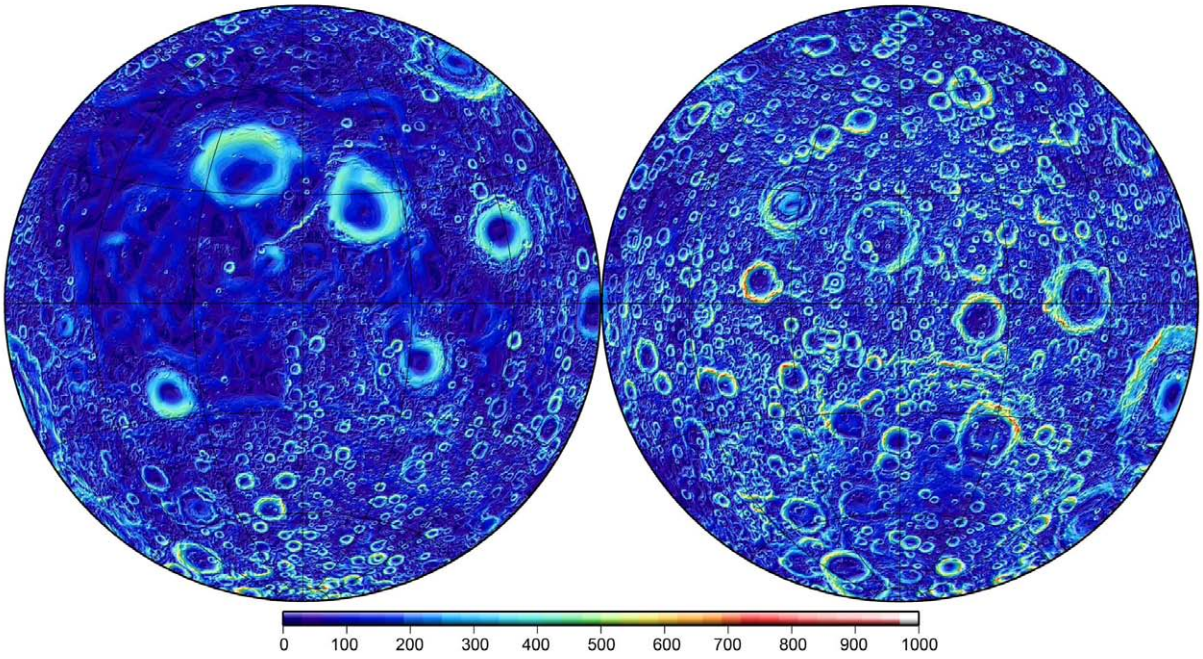

Figure 5. Magnitude of LGM2011 total vertical deflections at the lunar surface. Units in arc seconds.

Table 3. Descriptive statistics of LGM2011, SGM100i and LRTM70 vertical deflections in north-south (NS) and east-west (EW) directions. SGM100i deflections evaluated in band 2 to 70 at the surface of the LOLA topography. LRTM70 deflections obtained from Newtonian forward-modelling. LGM2011 deflections are the sum of SGM100i and LRTM70. Units in arc seconds.

Functional	**Min**	**Max**	**Mean**	**STD**
LGM2011 surface NS vertical deflection	-939	815	2	136
SGM100i NS vertical deflection	-552	534	2	102
LRTM70 NS vertical deflection	-583	555	0	89

LGM2011 surface EW vertical deflection	-838	768	0	129
SGM100i EW vertical deflection	-472	534	0	94
LRTM70 EW vertical deflection	-552	554	0	89

5. LGM2011 model verification

5.1 Implicit validation

Implicit validation of LGM2011 comes from the fact that Newtonian forward-modelling has been used successfully in the construction and augmentation of Earth gravity field models. Over regions devoid of high-resolution ground gravity, Pavlis et al. (2007) derived gravity from band-limited topography at spatial scales of ~30 km to ~10 km for the construction of a recent Earth gravity model. Over study areas in the European Alps (Switzerland, Bavaria), Newtonian forward-modelling was applied to estimate the gravity field at spatial scales of ~10 km down to ~100 m (Hirt, 2010; Hirt et al., 2010a, 2010b, 2011). This improved the agreement with ground-truth observations on the Earth's surface by ~50 % in the case of geoid undulations (Hirt et al., 2010a), 80 % in the case of vertical deflections (Hirt, 2010) and ~89 % in the case of gravity accelerations (Hirt et al., 2011). Importantly, the LGM2011 methodology (Section 2) is an exact replication of these strategies used in Earth gravity field refinement. The suitability of the forward-modelling approach for short-scale refinement of lunar gravity fields, as is the case with LGM2011, is therefore demonstrated implicitly.

5.2 Validation with measured gravity

As an explicit validation, LGM2011 was compared with measured gravity accelerations at the landing sites of the Apollo 11, 12, 14 (Nance, 1969, 1971a, 1971b) and Apollo 17 (Talwani, 2003) lunar surface missions (Table 4). The accuracy of Apollo 11 and 12 surface gravity is estimated to be 30 mGal (Nance, 1971a), Apollo 14 gravity to be better than 30 mGal (Nance, 1971b), while the Apollo 17 measurement uncertainty is 5 mGal (Talwani, 2003). Three out of these four lunar gravity measurements are located in flat terrain (small topography-generated gravity field signals at short scales), only one measurement (Apollo 17) can be safely assumed to have ground-truth quality, and there are no observations available over the rugged far-side.

Table 4. Apollo landing site coordinates (Davies et al., 1987) and measured gravity values (Nance, 1971a, 1971b; Talwani, 2003). 10^{-5} ms^{-2} = 1 mGal.

Landing Site	**Selenocentric latitude [°]**	**Selenocentric longitude [°]**	**Measured surface gravity [10^{-5} ms^{-2}]**	**Measurement uncertainty [10^{-5} ms^{-2}]**
Apollo 11	0.673	23.473	162852	~30
Apollo 12	-3.008	-23.425	162674	~30
Apollo 14	-3.644	-17.477	162653	<30
Apollo 17	20.192	30.765	162695	~5

From Table 5, the residuals between Apollo gravity observations and LGM2011 are at the level of few tens of mGal. These comparisons show that the Newtonian forward-modelling component improves the fit in three cases. Newtonian forward-modelling yields only minor improvements over flat terrain (Apollo landing sites 11, 12 and 14), as would be expected. For the Apollo 17 landing site located in the rugged Taurus-Littrow valley, the discrepancy diminishes from -82 mGal to +10 mGal (Table 5)

Table 5. Comparison between Apollo surface gravity observations and gravity from LGM2011 and variants. LGM2011* is the LGM2011 model without the Newtonian gravity (= SGM100i band 2 to 70 plus normal gravity from LGM2011). LP150Q* denotes the gravity from LP150Q (band 2 to 150) plus normal gravity from LGM2011. Units in mGal (10^{-5} ms^{-2}).

Mission	**LGM2011**	**Observed-LGM2011**	**LGM2011***	**Observed-LGM2011***	**LP150Q***	**Observed-LP150Q***
Apollo 11	162801	51	162792	60	162792	60
Apollo 12	162700	-26	162695	-21	162689	-15
Apollo 14	162621	32	162610	43	162647	6
Apollo 17	162685	10	162777	-82	162740	-45

We also compared the Apollo gravity observations with the satellite-derived LP150Q (Konopliv et al., 2001) in spectral bands 2 to 150 (Table 5), indicating that LGM2011 gravity is of widely comparable quality over flat terrain. The smaller residual with respect to the Apollo 17 gravity measurement is an indication that LGM2011 may be a better source of gravity in rugged terrain, but this cannot be proven based just on a single data point. The Apollo 17 comparison indicates that Newtonian forward-modelling is most effective in

mountainous regions, as is known from similar studies on Earth (Hirt, 2010; Hirt et al., 2010a). Given the uncertain gravity observations from Apollo 11, 12 and 14 and the fact LGM2011 is not capable of modelling the effects of local mass-density anomalies and isostatic compensation at spatial scales shorter than ~78 km, the agreement between observation and model is a satisfactory check on LGM2011.

5.3 Validation with LP150Q gravity

We have additionally verified the Newtonian approach by creating a band-limited gravity field model from LOLA spherical harmonic topography between degrees 71 and 120 (spatial scales of ~78 km to ~45 km) over a 30° x 30° tile south of Mare Serenitatis, where significant gravity signals are generated by the rugged topography. Because this test area (centred on -15°S, 15°W) is on the near-side of the Moon, LP150Q can be used for comparison in the same spectral band.

From Figs. 6A and 6B, the band-limited LP150Q and Newtonian gravity signals bear a strong resemblance, with a correlation coefficient as high as +0.94. The band-limited LP150Q gravity signal RMS of ~42 mGal drops to ~16 mGal when subtracting Newtonian gravity (61% reduction; Fig 6C). This comparison also demonstrates the successful recovery of topography-generated gravity signals by LP tracking-data in the chosen band and provides a check on the Newtonian gravity and vice versa. The differences shown in Fig. 6C are likely to reflect localised mass-density or compensation effects not accounted for by our forward-modelling, but also the more noisy high-degree terms of LP150Q.

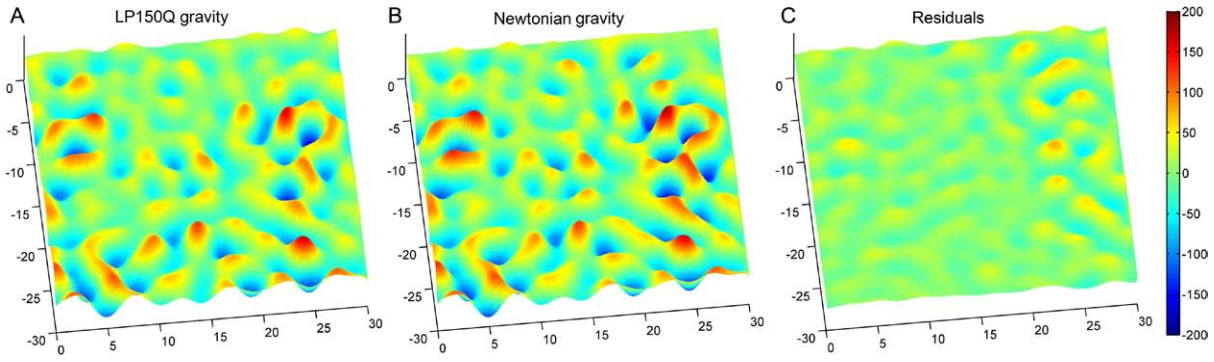

Figure 6. A: LP150Q gravity. B: Gravity from Newtonian forward-modelling. C: Residuals (LP150Q minus forward-modelling). Spectral band is from spherical harmonic degree 71 to 120, Units in 10^{-5} ms^{-2}.

6 Accuracy estimation

In the absence of dense gravity data sets of ground-truth quality on the lunar surface, estimation of the LGM2011 accuracy is not straightforward. The above comparison with the four available ground observations and LP150Q gravity suggest that LGM2011 provides lunar surface gravity accurate to some 10s of mGal. An exact error estimate is difficult to determine from only four data points, especially as the uncertainty of the ground truth is around 30 mGal in three cases.

Variations of ~25 mGal over few km have been reported for Bouguer gravity anomalies near the Apollo 17 landing site (Talwani, 2003), indicating the minimum discrepancies to be expected between the 'true' gravity (as could be measured with gravimeters on the lunar surface) and LGM2011 gravity that relies on the isostatic uncompensation and constant density assumptions at scales less than ~78 km. Crucially, the accuracy of LGM2011 surface gravity accelerations depend on the agreement between the LOLA-implied terrain and real lunar surface. An elevation error of 100 m translates into ~19 mGal free-air gravity effect (Section 2.3). Opposed to this, LGM2011 free-air gravity anomalies are not subject to this error source.

LGM2011 vertical deflections are cautiously estimated to be accurate to few 10 arc seconds, but this cannot be proven in the absence of ground-truth observations. From Sections 4 and 5, we are confident that LGM2011 functionals generally approximate the true lunar gravity field more accurately than truncated space-collected models, particularly over rugged parts of the lunar surface.

7 Applications and limitations

Given that LGM2011 does not incorporate gravity-field observations beyond degree 70, we do not recommend it for direct geophysical or geological interpretation at shorter scales. At spatial scales shorter than 78 km, LGM2011 relies on the assumption of uncompensated and constant mass-density topography, so does not offer information on gravity signatures departing from these assumptions (cf. Section 2.3). Nonetheless, LGM2011 significantly improves upon the resolution of existing lunar gravity fields and can be expected to approximate the entire spectrum of the lunar gravity field reasonably well. This is backed up by experiences from Earth, the comparisons with lunar surface gravity observations (Table 5) and the near-side comparison with the band-limited LP150Q (Figure 6). Because of its resolution, LGM2011 is beneficial for gravity field modelling efforts and engineering applications, where the full spectral resolution of lunar gravity is sought.

LGM2011 can be used favourably for lunar gravity field simulation and as an a-priori model for geophysical inversion studies. Specifically, we anticipate that LGM2011 and LRTM70 will be of value to the GRAIL mission (Zuber et al., 2011; Hoffman, 2009). GRAIL aims to produce a lunar gravity field to scales of ~27 km (Zuber et al., 2011), or spherical harmonic degree 180. For instance, the topography-implied gravity field could be used for calibration of GRAIL gravity measurements and for mutual comparisons with future GRAIL gravity field models. On the one hand, we expect GRAIL to provide a feedback on the LGM2011 assumption of uncompensated and constant-mass topography. On the other hand, comparisons with topography-implied gravity field maps (as in Fig. 6) can be useful to assess the GRAIL model quality in the spatial domain, specifically the mission's sensitivity to short-scale lunar gravity.

To engineering-driven applications, LGM2011 may be used in the context of future lunar exploration or landing missions, e.g., for the prediction of gravity accelerations at prospective lunar landing sites and comparisons with future gravity measurements at the lunar surface. For future inertial navigation upon or close to the lunar surface, LGM2011 vertical deflections may prove useful to correct for the effects of the short-wavelength anomalous gravity field (cf. Grejner-Brzezinska and Wang, 1998).

The new high-resolution topography models (e.g., from ongoing LOLA laser altimetry), require accurate selenoid undulations to provide physically meaningful heights. As physical height reference surface, the selenoid is crucial in the analysis of gravity-driven processes, e.g., the study of basalt flow directions, see Wieczorek (2007). Due to limited resolution, conventional lunar gravity fields to degree 70 do not represent the short-scale gravity field, which, in case of selenoid undulations has a signal strength of ~10 m and range of ~100 m. With our LRTM70 selenoid product, the selenoid's fine-structure can now be taken into account. Also, the construction of accurate LOLA topography models requires precise knowledge (at the 1m-level in the radial direction) of the LRO orbit (Mazarico et al., 2010). According to Mazarico et al. (2010), this orbit requirement will "*necessitate new solutions of the lunar gravity field in order to model short-wavelength gravity anomalies not necessarily captured by current solutions.*" Upward-continued LRTM70 selenoid undulations may prove beneficial to reduce gravity-field-induced short-scale perturbations of the LRO orbit, particularly over the rugged far-side.

Our LGM2011 model may be used to study the expected spectrum of the entire lunar gravity field, down to unprecedented km-scales. Further to this, scientists are interested to know the variability of gravity field functionals over the entire lunar surface (cf. Sagitov et

al., 1986). LGM2011 provides much improved knowledge of the expected variations in surface gravity, free-air gravity anomalies and vertical deflections in comparison to earlier efforts, e.g., by Sagitov et al. (1986).

8 Concluding Remarks

LGM2011 is the first-ever model to resolve the lunar gravity field down to km-scales. Constructed as composite of space-collected and topography-implied gravity, LGM2011 is the spectrally most complete description of the entire lunar gravity field to date. The use of topography data to estimate the expected gravity field fine-structure (LRTM70) relies on the assumptions of uncompensated topography and constant mass-density, which is why effects departing from these assumptions are not modelled beyond harmonic degree 70. Thus, LGM2011 or LRTM70 cannot be recommended for direct geological interpretation at spatial scales less than ~78 km

LGM2011 is constructed based on the same principles used successfully in short-scale Earth gravity field modelling. Based on these experiences and our verification experiments presented herein, we expect LGM2011 and LRTM70 to approximate the true lunar gravity field reasonably well at scales down to ~1.5 km. This opens a range of new applications in gravity field modelling, validation and statistical analysis. In view of current and future lunar exploration efforts, engineering-driven applications are expected to benefit from LGM2011.

The LGM2011 and LRTM70 models are provided at 0.05° resolution over the entire lunar surface. The complete set of LGM2011 surface gravity accelerations and free-air anomalies, the LGM2011 input data sets and the by-products of selenoid undulations and vertical deflections are freely available from http://www.geodesy.curtin.edu.au/research/models/lgm2011/ and are provided as Electronic Supplementary Material to this article.

Acknowledgements

We thank the Australian research council for funding through Discovery Project Grant DP0663020. We also gratefully thank the reviewers, particularly reviewer #1, and editor for helping us to clarify many points because of their very thorough attention to detail.

Author contributions Both authors formulated and designed this study. C.H. carried out the computations and analyses. Both authors discussed the results and contributed to writing the paper.

References

Araki, H., Tazawa, S., Noda, H., Ishihara, Y., Goossens, S., Sasaki, S., Kawano, N., Kamiya, I., Otake, H., Oberst, J., Shum, C.K., 2009. Lunar global shape and polar topography derived from Kaguya-LALT laser altimetry. Science 323(5916), 897-900, doi: 10.1126/science.1164146.

Davies, M.E., Colvin, T.R., Meyer, D.L., 1987. A Unified Lunar Control Network: The Near Side. J. Geophys. Res., 92(B13), 14177–14184.

Forsberg, R., Tscherning, C.C., 1981. The use of height data in gravity field approximation by collocation. J. Geophys. Res. 86(B9), 7843-7854.

Forsberg, R., 1984. A study of terrain reductions, density anomalies and geophysical inversion methods in gravity field modelling. Report 355, Department of Geodetic Science and Surveying, Ohio State University, Columbus.

Goossens, S., Visser, P.N.A.M., Heki, K., Ambrosius, B.A.C., 2005. Local gravity from Lunar Prospector tracking data: results for Mare Serenitatis. Earth Planets Space 57, 1127–1132.

Goossens, S., Matsumoto, K., Liu, Q., Kikuchi, F., Sato, K., Hanada, H., Ishihara, Y., Noda H., Kawano, N., Namiki, N., Iwata, T., Lemoine, F.G., Rowlands, D.D., Harada, Y., Chen, M., 2011. Lunar gravity field determination using SELENE same-beam differential VLBI tracking data. J. Geod., 85, 205-228, DOI 10.1007/s00190-010-0430-2.

Grejner-Brzezinska, D.A., Wang, J., 1998. Gravity Modeling for High-Accuracy GPS/INS Integration. Navigation, 45, 3, 209-220.

Han, S.C., Mazarico, E., Rowlands, D., Lemoine, F., Goossens, S., 2011. New analysis of Lunar Prospector radio tracking data brings the nearside gravity field of the Moon with an unprecedented resolution, Icarus, 215(2), 455-459, 10.1016/j.icarus.2011.07.020.

Hirt, C., 2010. Prediction of vertical deflections from high-degree spherical harmonic synthesis and residual terrain model data. J. Geod. 84(3), 179–190, doi: 10.1007/s00190-009-0354-x.

Hirt, C., Featherstone, W.E., Marti, U., 2010a. Combining EGM2008 and SRTM/DTM2006.0 residual terrain model data to improve quasigeoid computations in mountainous areas devoid of gravity data. J. Geod. 84(9), 557-567, doi: 10.1007/s00190-010-0395-1.

Hirt, C., Marti, U., Bürki, B., Featherstone, W.E., 2010b. Assessment of EGM2008 in Europe using accurate astrogeodetic vertical deflections and omission error estimates from SRTM/DTM2006.0 residual terrain model data. J. Geophys. Res. 115, B10404, DOI:10.1029/2009JB007057.

Hirt, C., Gruber, T., Featherstone, W.E., 2011. Evaluation of the first GOCE static gravity field models using terrestrial gravity, vertical deflections and EGM2008 quasigeoid heights. J Geod, 85(10): 723-740, doi: 10.1007/s00190-011-0482-y.

Hoffman, T.L., 2009. GRAIL: Gravity Mapping the Moon. Proceedings of the 2009 IEEE Aerospace Conference, Big Sky, MT, USA, March 7-14, 2009, Vols. 1-7, 293-300.

Holmes, S.A., Pavlis, N.K., 2008. Spherical harmonic synthesis software harmonic_synth. http://earth-info.nga.mil/GandG/wgs84/gravitymod/new_egm/new_egm.html. Last accessed on 01.05.2011.

JPL, 2005. Lunar constants and models document. JPL D-32296. Jet Propulsion Laboratory, Pasadena, USA.

Kaula, W.M., 1966. Theory of Satellite Geodesy. Blaisdel, Waltham.

Konopliv, A.S., Binder, A.B., Hood, L.L., Kucinskas, A.B., Sjogren, W.L., Williams, J.G., 1998. Improved gravity field of the Moon from Lunar Prospector. Science 281(5382), 1476-1480, doi: 10.1126/science.281.532.1476.

Konopliv, A.S., Asmar, S.W., Carranza, E., Sjogren, W.L., Yuan, D.N., 2001. Recent gravity models as a result of the Lunar Prospector mission. Icarus 150(1), 1-18, doi:10.1006/icar.2000.6573.

Matsumoto, K., Goossens, S., Ishihara, Y., Liu, Q., Kikuchi, F., Iwata, T., Namiki, N., Noda, H., Hanada, H., Kawano, N., Lemoine, F.G., Rowlands, D.D., 2010. An improved lunar gravity field model from SELENE and historical tracking data: Revealing the farside gravity features. J. Geophys. Res. 115, E0600, doi:10.1029/2009JE003499.

Mazarico, E., Lemoine, F.G., Han, S.C., Smith, D.E., 2010. GLGM-3: A degree-150 lunar gravity model from the historical tracking data of NASA Moon orbiters. J. Geophys. Res. 115, E05001, doi:10.1029/2009JE003472.

Nagy, D., Papp, G., Benedek, J., 2000. The gravitational potential and its derivatives for the prism. J. Geod. 74(7-8), 552–560. doi: 10.1007/s001900000116. Erratum in 76(8):475. doi: 10.1007/s00190-002-0264-7.

Namiki, N., Iwata, T., Matsumoto, K., Hanada, H., Noda, H., Goossens, S., Ogawa, M., Kawano, N., Asari, K., Tsuruta, S., Ishihara, Y., Liu, Q., Kikuchi, F., Ishikawa, T., Sasaki, S., Aoshima, C., Kurosawa, K., Sugita, S., Takano, T., 2009. Farside gravity field of the Moon from four-way Doppler measurements of SELENE (Kaguya). Science 323(5916), 900-905, doi: 10.1126/science.1168029.

Nance, R.L., 1969. Gravity: First Measurement on Lunar Surface. Science 166: 384.

Nance, R.L., 1971a. Gravity measured at the Apollo 12 landing site. Phys. Earth Planet. Inter. 4, 193-196.

Nance, R.L., 1971b. Gravity measured at the Apollo 14 landing site. Science 174, 1022.

Pavlis, N.K., Factor, J.K., Holmes, S.A., 2007. Terrain-related gravimetric quantities computed for the next EGM. Proceedings of the 1st International Symposium of the International Gravity Field Service (IGFS), Istanbul, pp 318-323.

Reindler, L., Arkani-Hamed, J., 2001. The compensation state of intermediate size lunar craters, Icarus 153: 71-88, doi: 10.1006/icar.2001.6677.

Rowlands, D.D., Lemoine, F.G., Chinn, D.S., Luthcke, S.B., 2009. A simulation study of multi-beam altimetry for lunar reconnaissance orbiter and other planetary missions. J. Geod. 83(8), 709-721, doi: 10.1007/s00190-008-0285-y.

Sagitov, M.U., Bodri, B., Nazarenko, V.S., Tadzhidinov, K.G., 1986. Lunar Gravimetry. Academic Press, Orlando, Florida, ISBN 0126146608.

Seidelmann, P.K., Abalakin, V.K., Bursa, M., et al., 2002. Report Of The IAU/IAG Working Group On Cartographic Coordinates And Rotational Elements Of The Planets and Satellites: 2000. Celestial Mechanics and Dynamical Astronomy 82, 83-110.

Sinha, M., Gopinath, N.S., Malik, N.K., 2010. Lunar gravity field modelling: critical analysis and challenges. Adv. Space Res. 45(2): 322-349. doi:10.1016/j.asr.2009.10.006.

Smith, D.E., Zuber, M.T., Neumann, G.A., Lemoine, F.G., et al., 2010. Initial observations from the Lunar Orbiter Laser Altimeter (LOLA). Geophys. Res. Lett. 37, L18204, doi: 10.1029/2010GL043751.

Sugano, T., Heki, K., 2004a. High resolution lunar gravity anomaly map from the lunar prospector line-of-sight acceleration data. Earth Planets Space 56, 81–86.

Sugano, T., Heki, K., 2004b. Isostasy of the Moon from high-resolution gravity and topography data: Implication for its thermal history. Geophys. Res. Lett. 31: L24703, doi:10.1029/2004GL022059.

Talwani, M., 2003. The Apollo 17 gravity measurements on the Moon. The Leading Edge August 2003, 786.

Torge, W., 2001. Geodesy. Third edition, de Gruyter, Berlin.

Vondrak, R., Keller, J., Chin, G., Garvin, J., 2010. Lunar Reconnaissance Orbiter (LRO): observations for Lunar exploration and science. Space Science Rev. 150: 7-22, doi: 10.1007/s11214-010-9631-5.

Watts, A.B., 2001. Isostasy and Flexure of the Lithosphere. Cambridge University Press.

Wieczorek, M.A., 2007. Gravity and topography of the terrestrial planets. In: Spohn, T., Schubert, G. (Eds.), Treatise on Geophysics, vol. 10. Elsevier–Pergamon, Oxford, pp. 165–206.

Zuber, M.T., Smith, D.E., Watkins, M., and the GRAIL Science Team, 2011. The GRAIL Discovery Mission for Launch Sept 2011. EGU General Assembly 2011,Geophys. Res. Abst., Vol. 13, EGU2011-4264-1, 2011.